Journal of Heat and Mass Transfer Research

Journal homepage: https://jhmtr.semnan.ac.ir

Semnan University

ISSN: 2383-3068

Research Article

Entropy Generation of Two Immiscible Fluid Flow of Couple-Stress and Viscous Liquid in a Vertical Wavy Porous Space

J. Bala Anasuya *, **Suripeddi Srinivas**

School of Advanced Sciences, VIT-AP University, Inavolu, Amaravath, 522237, India

ARTICLE INFO

Article history:

Received: 2023-10-27

Revised: 2024-03-17

Accepted: 2024-03-17

Keywords:

Wavy channel;
Travelling thermal waves;
Brikman number;
Couple - Stress fluid;
Bejan number.

ABSTRACT

The purpose of this research is to examine the entropy generation analysis of two immiscible MHD fluid flows in a vertical wavy channel with travelling thermal waves and porous space when subjected to an external magnetic field. Region-I is occupied with a couple-stress liquid, while region-II is with viscous liquid. The wall channels are maintained at different temperatures and concentrations. The governing flow equations are derived by taking into account the presence of both a mean part and a perturbed part in the solution. Long wave approximation, which contributes to the wall waviness, is used to derive the solution of the perturbed part. The R-K 4th-order method is employed together with the shooting technique to solve the resultant system of coupled and non-linear ordinary differential equations. The results are presented graphically for the distribution of velocity, heat, and concentration, entropy generation, Bejan number, shear stress, Nusselt number, and Sherwood number for arising parameters, Hartmann number, Brinkman number, porous parameter, couple-stress parameters, waviness parameter, Schmidt number, and Soret number and are discussed. As the couple stress fluid parameter, Grashoff number, and heat generation/absorption increase, the velocity distribution rises. Temperature drops as the porosity parameter and Hartmann number increase. With a rise in the Soret and Schmidt numbers, concentration reduces. Entropy generation decreases with the Hartmann number, porous parameter, and chemical reaction parameter and increases with the Brinkman number. The numerical solutions obtained are compared with previously published work to validate the model, and the results exhibit a remarkable agreement.

1. Introduction

Due to its numerous uses in industry and engineering, the two-phase liquid flows through channels or over-moving surfaces have gained a great deal of attention in recent years. Such flows are utilized in industrial processes and techniques for transporting multiphase liquids via conduits and wells. Oil-water mixes flow through pipelines and channels, and in mass transfer systems, the extraction of liquid-liquid solvents are some more applications of two-phase flow.

Fluid flow via the channels of wavy walls has captured the attention of researchers owing to its practical uses in re-entry vehicles and rocket booster transpiration cooling, cross-hatching on ablative surfaces, and film vaporisation in combustion chambers. Wavy-walled surfaces are a method for meeting industrial requirements in small heat exchangers to increase heat transfer rates. In medical treatments, wavy walls are widely utilised to increase mass transport (blood oxygenator). The combination of two or more sinusoidal surfaces creates a complicated wavy

* **Corresponding author.**
E-mail address: bala2043@gmail.com

Cite this article as:
Anasuya, J.B. and Srinivas, S., 2024. Entropy Generation of Two Immiscible Fluid Flow of Couple-Stress and Viscous Liquid in a Vertical Wavy Porous Space. *Journal of Heat and Mass Transfer Research*, 11(1), pp. 109-126.
https://doi.org/10.22075/JHMTR.2024.32180.1490

surface that may transport heat more quickly than a single sinusoidal surface. Shankar and Sinha [1] have performed in-depth research on the Rayleigh problem for a wavy wall and obtained some exciting results. Lessen and Gangwani [2] analysed the effects of small amplitude wall waviness on the laminar boundary layer stability. The MHD flow with combined free and forced convection in vertical channels with wavy walls along with traveling thermal waves was studied by Vajravelu [3]. Investigation into the natural convection heat transmission in vertical wavy channels was done by Vajravelu and Sastri [4]. Muthuraj and Srinivas [5] investigated the effects of viscous dissipation and space porosity in a wavy channel when fluid is subjected to a magnetic field. Umavathi and Shekar [6] presented the analytical results for a mixed convective flow of two immiscible liquids in a vertical channel with wavy walls and traveling thermal waves. The investigation pertaining to heat and mass transfer characteristics of an unsteady flow of two immiscible liquids between flat and long wavy vertical walls has been reported by Umavathi et al. [7].

Modern technology and industry are relying increasingly on non-Newtonian fluids, and a quantum of research has been done specifically in this domain. The study of the couple- stress liquid, of the category of non-Newtonian fluid, has become increasingly important as it has distinctive features like polar effects that possess the mechanism that describes the complex behaviour of fluids like liquid crystals and human blood in lubrication theory. Stokes (1966) introduced the couple- stress fluid. This fluid is a generalisation of the traditional theory of viscous liquids. The consequences of couple-stress flow in a squeeze film were examined by Bujurke and Jayaraman [8], with particular attention paid to synovial joints. According to their findings, the squeeze film time of a couple-stress liquid is longer than that of a Newtonian liquid of the same viscosity. Rudraiah and Chandrashekara [9] investigated the impact of couple-stress liquid on Rayleigh-Taylor instability control at the interface of a dense liquid driven by a lighter liquid. The effect of several types of basic temperature gradients of couple-stress fluid-saturated porous media was studied by Shivakumara et al. [10]. The double-diffusive free convective flow of a couple-stress liquid with the influence of Soret and Dufour's effects was reported by Rani and Reddy [11]. Zeeshan, Ahmed, et al. [12] explore the flow of non-Newtonian couple-stress fluid in two dimensions across the upper horizontal surface of a paraboloid (uhsp), which is shaped like a submarine or any other aerodynamic vehicle. Umavathi et al.[13] investigated fully developed laminar flow between vertical parallel plates in a composite porous medium with two immiscible viscous and couple-stress liquids. Srinivas and Ramana Murthy [14] explored the flow of two immiscible, incompressible couple-stress fluids between two permeable beds under the influence of a constant pressure gradient. The two-phase flow of couple-stress and viscous liquids in an inclined channel was reported by Abbas et al. [15]. Heat and mass transfer effects on the oscillatory flow of a couple-stress liquid in a wavy channel were analysed by Lawanya et al.[16]. Adenasya [17] examined the influence of radiative heat transfer on oscillatory MHD non-Newtonian couple-stress liquid flow through a vertical porous channel with non-uniform wall temperature resulting from periodic heat input at the heated wall. Bashir Sammar and Muhammad Sajid [18] explored the flow of two uniformly rotating immiscible couple-stress fluid layers. The convection process occurs naturally in situations where the combined effects of heat and concentration buoyancy exist, such as heat exchangers, petroleum reservoirs, fire engineering, and nuclear energy combustion modeling. The combined action of heat and chemical diffusion provides the flow through the driving forces in various transport process applications, including solar energy collectors, thermal protection systems, and chemical distilleries. Mixed convection flows with heat and mass transfer through a magnetic field, and chemical reactions are observed in various transport processes across numerous scientific and engineering disciplines. In the chemical and hydrometallurgical industries, the study of heat and mass transfer with chemical reactions is of greatest significance. Srinivasacharya [19] investigated the Soret and Dufour effects on natural convection heat and mass transport of a couple-stress liquid in a vertical channel with the chemical reaction. Srinivas and Muthuraj [20] studied hydromagnetic mixed convective heat and mass transfer peristaltic flow with a chemical reaction in a porous vertical space. Hayat et al. [21] investigated the Soret and Dufour effects on MHD peristaltic flow of a couple-stress fluid in an inclined channel under the influence of Joule heating and chemical reaction. Very recently, Padma and Srinivas [22] investigated the combined effects of Hall current, thermal radiation, heat source, and chemical reaction on heat and mass characteristics in a vertical porous channel filled with a two-layered viscoelastic liquid under the influence of a periodic pressure gradient. Most recently, the hydromagnetic pulsating flow of two immiscible liquid layers with joule heating and first-order chemical reaction was reported by Goyal and Srinivas [23].

Entropy generation is used in nuclear reactors, cooler heat engines and pumps, and solar energy systems. To prevent the loss of heat energy because of the efficiency of the energy orientation system and to optimize the process, irreversible energy is required in the thermal system as much as possible. Several researchers have conducted theoretical and experimental research on entropy generation and proposed that entropy production can be minimised by selecting the appropriate fluid flow models. Adenasya et al. [24] have studied the second law analysis for a reactive couple-stress liquid flowing through a porous channel.

Janardhan Reddy et al. [25] investigated the entropy heat production analysis for unsteady MHD couple-stress fluid flow over a uniformly heated vertical flat plate.

Srinivas et al. [26] analysed the entropy generation of a steady flow of two immiscible couple-stress liquids in a horizontal channel with two porous beds.

Thota Siva [27] studied the electroosmotic and electromagnetohydrodynamic transport of couple-stress liquid in a microchannel in order to predict the flow dynamics, thermal transport, and entropy generation in a thermo fluidic system with slip-dependent zeta potential.

Though there are a large number of studies on two immiscible flows in a vertical channel (tube), very few studies on the two immiscible flows in a vertical wavy channel have been reported in the literature.

To the authors' knowledge, no research has been done on the MHD mixed convective heat and mass transfer analysis of two immiscible couple-stress fluids and viscous fluids in a vertical wavy channel with a chemical reaction.

Therefore, the main goal is to construct a mathematical model to understand the effect of heat and mass transfer on the MHD of two immiscible fluid flows in a vertical wavy porous space, with the flow induced by traveling thermal waves in the presence of a chemical reaction.

One region is occupied with couple-stress liquid, and another region is filled with viscous liquid. Flow properties, as well as heat and mass transfer characteristics, are analyzed by plotting graphs and discussed in detail by varying parameters like Hartmann number, Brinkmann number, Grashof number, local Grashof number, porous parameter, couple-stress parameter, thermal radiation, and heat generation (absorption) and Bejan number.

Also, the Nusselt number, Sherwood number, and Shear stress at the walls are presented graphically.

2. Flow Geometry

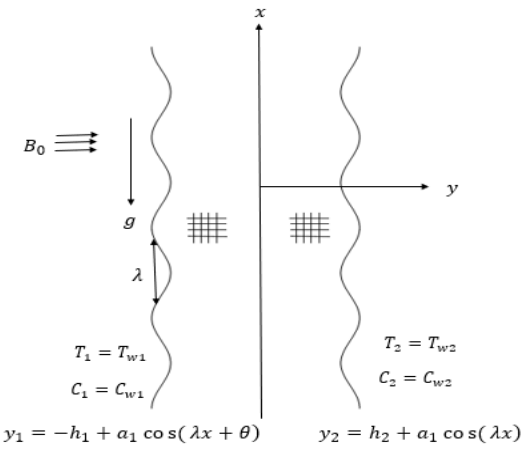

Fig. 1. Sketch of the model

3. Mathematical Formulation

Consider the laminar motion of two layered immiscible flow in a vertical wavy porous space (Fig. 1).

Region – I: $-h_1 \le y \le 0$, is filled with couple-stress liquid.

Region – II: $0 \le y \le h_2$ is occupied by clear viscous liquid. $y = -h_1 + a_1 \cos(\lambda x + \theta)$ and $y = h_2 + a_1 \cos(\lambda x + \theta)$ are the left and right wavy walls of the channel, where a_1 is the amplitude of the wave and λ is wave number.

The liquids in both regions are different with different physical properties. Both the channel boundaries are held at different temperatures. The govering equations are given by [13 & 14].

Region-I

$$\frac{\partial u_1}{\partial x} + \frac{\partial v_1}{\partial y} = 0, \tag{1}$$

$$\rho_1\left(\frac{\partial u_1}{\partial t} + u_1\frac{\partial u_1}{\partial x} + v_1\frac{\partial u_1}{\partial y}\right) = -\frac{\partial p_1}{\partial x} + \mu_1\left(\frac{\partial^2 u_1}{\partial x^2} + \frac{\partial^2 u_1}{\partial y^2}\right) - \eta\left(\frac{\partial^2}{\partial x^2} + \frac{\partial^2}{\partial y^2}\right)u_1 - \frac{\mu}{k}u_1 - \sigma B_0^{\,2}u_1 + \rho_1 g\beta_{t1}\left(T_1 - T_{w1}\right) + \rho_1 g\beta_{c1}\left(C_1 - C_{w1}\right) \tag{2}$$

$$\rho_1\left(\frac{\partial v_1}{\partial t} + u_1\frac{\partial v_1}{\partial x} + v_1\frac{\partial v_1}{\partial y}\right) = -\frac{\partial p_1}{\partial y} + \mu_1\left(\frac{\partial^2 v_1}{\partial x^2} + \frac{\partial^2 v_1}{\partial y^2}\right) - \eta\left(\frac{\partial^2}{\partial x^2} + \frac{\partial^2}{\partial y^2}\right)v_1 - \frac{\mu}{k}v_1 \tag{3}$$

$$\rho_1 cp\left(\frac{\partial T_1}{\partial t}+u_1\frac{\partial T_1}{\partial x}+v_1\frac{\partial T_1}{\partial y}\right)=k_1\left(\frac{\partial^2 T_1}{\partial x^2}+\frac{\partial^2 T_1}{\partial y^2}\right)$$
$$+\mu_1\left\{2\left[\left(\frac{\partial u_1}{\partial x}\right)^2+\left(\frac{\partial v_1}{\partial y}\right)^2\right]+\left(\frac{\partial u_1}{\partial y}+\frac{\partial v_1}{\partial x}\right)^2\right\}$$
$$+\eta\left[\left(\frac{\partial^2 v_1}{\partial x^2}+\frac{\partial^2 v_1}{\partial y^2}\right)^2+\left(\frac{\partial^2 u_1}{\partial x^2}+\frac{\partial^2 u_1}{\partial y^2}\right)^2\right] \quad (4)$$
$$+Q\left(T_1-T_{w1}\right)-\frac{\partial q_1}{\partial y}$$

$$\left(\frac{\partial C_1}{\partial t}+u_1\frac{\partial C_1}{\partial x}+v_1\frac{\partial C_1}{\partial y}\right)=D_1\left(\frac{\partial^2 C_1}{\partial x^2}+\frac{\partial^2 C_1}{\partial y^2}\right)$$
$$+\frac{D_1K_T}{T}\left(\frac{\partial^2 T_1}{\partial x^2}+\frac{\partial^2 T_1}{\partial y^2}\right)-\gamma_1\left(C_1-C_{w1}\right) \quad (5)$$

Region –II

$$\frac{\partial u_2}{\partial x}+\frac{\partial v_2}{\partial y}=0, \quad (6)$$

$$\rho_2\left(\frac{\partial u_2}{\partial t}+u_2\frac{\partial u_2}{\partial x}+v_2\frac{\partial u_2}{\partial y}\right)=-\frac{\partial p_2}{\partial x}$$
$$+\mu_2\left(\frac{\partial^2 u_2}{\partial x^2}+\frac{\partial^2 u_2}{\partial y^2}\right)-\frac{\mu}{k}u_2-\sigma {B_0}^2u_2 \quad (7)$$
$$+\rho_2 g\beta_{t2}\left(T_2-T_{w2}\right)+\rho_2 g\beta_{c2}\left(C_2-C_{w2}\right)$$

$$\rho_2\left(\frac{\partial v_2}{\partial t}+u_2\frac{\partial v_2}{\partial x}+v_2\frac{\partial v_2}{\partial y}\right)=-\frac{\partial p_2}{\partial y}$$
$$+\mu_2\left(\frac{\partial^2 v_2}{\partial x^2}+\frac{\partial^2 v_2}{\partial y^2}\right)-\frac{\mu}{k}v_2 \quad (8)$$

$$\rho_2 cp\left(\frac{\partial T_2}{\partial t}+u_2\frac{\partial T_2}{\partial x}+v_2\frac{\partial T_2}{\partial y}\right)=k_2\left(\frac{\partial^2 T_2}{\partial x^2}+\frac{\partial^2 T_2}{\partial y^2}\right)$$
$$+\mu_2\left\{2\left[\left(\frac{\partial u_2}{\partial x}\right)^2+\left(\frac{\partial v_2}{\partial y}\right)^2\right]+\left(\frac{\partial u_2}{\partial y}+\frac{\partial v_2}{\partial x}\right)^2\right\} \quad (9)$$
$$+Q\left(T_2-T_{w2}\right)-\frac{\partial q_2}{\partial y}$$

$$\left(\frac{\partial C_2}{\partial t}+u_2\frac{\partial C_2}{\partial x}+v_2\frac{\partial C_2}{\partial y}\right)=D_2\left(\frac{\partial^2 C_2}{\partial x^2}+\frac{\partial^2 C_2}{\partial y^2}\right)$$
$$+\frac{D_2K_T}{T}\left(\frac{\partial^2 T_2}{\partial x^2}+\frac{\partial^2 T_2}{\partial y^2}\right)-\gamma_2\left(C_2-C_{w2}\right) \quad (10)$$

where the conditions of the temperature and concentration on the walls are: [3,5,6]

$$T_1=\hat{T}_{w_1}\left(1+\varepsilon\cos\left(\lambda x+\omega t\right)\right)=T_{w_1}$$
$$T_2=\hat{T}_{w_2}\left(1+\varepsilon\cos\left(\lambda x+\omega t\right)\right)=T_{w_2}$$
$$C_1=\hat{C}_{w_1}\left(1+\varepsilon\cos\left(\lambda x+\omega t\right)\right)=C_{w_1}, \quad (11)$$
$$C_2=\hat{C}_{w_2}\left(1+\varepsilon\cos\left(\lambda x+\omega t\right)\right)=C_{w_2}$$

The conditions used at the boundary and interface are [6 & 15]

$$u_1=v_1=0, \quad y=-h_1+a_1\cos\left(\lambda x+\theta\right)$$
$$u_2=v_2=0, \quad y=h_2+a_1\cos\left(\lambda x\right)$$
$$u_1=u_2,\ v_1=v_2, \quad y=0,$$
$$\mu_1\left(\frac{\partial u_1}{\partial y}+\frac{\partial v_1}{\partial x}\right)-\eta\left(\frac{\partial^3 u_1}{\partial y^3}+\frac{\partial^3 v_1}{\partial x^3}\right)=\mu_2\left(\frac{\partial u_2}{\partial y}+\frac{\partial v_2}{\partial x}\right),\ y=0,$$
$$\frac{\partial p_1}{\partial x_1}=\frac{\partial p_2}{\partial x_2}, \quad y=0$$
$$\frac{\partial^2 u_1}{\partial y^2}=0,\ y=0,$$
$$\frac{\partial^2 u_1}{\partial y^2}=0,\ y=-h_1+a_1\cos\left(\lambda x+\theta\right), \quad (12)$$
$$T_1=T_{w1}, \quad y=-h_1+a_1\cos\left(\lambda x+\theta\right),$$
$$T_2=T_{w2}, \quad y=h_2+a_1\cos\left(\lambda x\right)$$
$$T_1=T_2, \quad y=0,$$
$$k_1\left(\frac{\partial T_1}{\partial y}+\frac{\partial T_1}{\partial x}\right)=k_2\left(\frac{\partial T_2}{\partial y}+\frac{\partial T_2}{\partial x}\right), \quad y=0$$
$$C_1=C_{w1}, \quad y=-h_1+a_1\cos\left(\lambda x+\theta\right),$$
$$C_2=C_{w2}, \quad y=h_2+a_1\cos\left(\lambda x\right)$$
$$C_1=C_2, \quad y=0,$$
$$D_1\left(\frac{\partial C_1}{\partial y}+\frac{\partial C_1}{\partial x}\right)=D_2\left(\frac{\partial C_2}{\partial y}+\frac{\partial C_2}{\partial x}\right), \quad y=0$$

Non dimensional quantities and pressure gradient are given by

$$u_1 = \frac{h_1}{\nu_1}u_1^*, v_1 = \frac{h_1}{\nu_1}v_1^*, u_2 = \frac{h_2}{\nu_2}u_2^*, v_2 = \frac{h_2}{\nu_2}v_2^*$$
$$, x_1 = \frac{x^*_1}{h_1}, y_1 = \frac{y^*_1}{h_1}, x_2 = \frac{x^*_2}{h_2}, y_2 = \frac{y^*_2}{h_2}, t_1 = \frac{t^*\nu_1}{h_1^2},$$
$$t_2 = \frac{t^*\nu_2}{h_2^2}, p_1 = \frac{p_1h_1^2}{\rho_1\nu_1^2}, p_2 = \frac{p_2h_2^2}{\rho_2\nu_2^2}, T_1 = \frac{T_1 - T_{w1}}{\Delta T},$$
$$T_2 = \frac{T_2 - T_{w2}}{\Delta T}, C_1 = \frac{C_1 - C_{w1}}{\Delta C}, C_2 = \frac{C_2 - C_{w2}}{\Delta C},$$
$$\beta = \frac{\beta_2}{\beta_1}, h = \frac{h_2}{h_1}, m = \frac{\mu_1}{\mu_2}, n = \frac{\rho_2}{\rho_1}, k = \frac{k_2}{k_1}, s = \frac{\sigma_2}{\sigma_1},$$
$$\nu_1 = \frac{\mu_1}{\rho_1}, \nu_2 = \frac{\mu_2}{\rho_2}, D = \frac{D_2}{D_1}, \gamma = \frac{\gamma_2}{\gamma_1}, \varepsilon = \frac{a_1}{h} \tag{13}$$

$$\lambda = \frac{\lambda^*}{h}, Gr_{t1} = \frac{h_1^3 g\beta_t\Delta T}{\upsilon^2}, Gr_{c1} = \frac{h_1^3 g\beta_c\Delta C}{\upsilon^2},$$
$$\sigma = \frac{h_1}{\sqrt{k}}, M^2 = \frac{\sigma_1}{\rho_1\upsilon_1}, a^2 = \frac{\rho_1\upsilon_1h_1^2}{\eta},$$
$$Gr_{t2} = Gr_{t1}\beta^2h^3n^2m^2, Gr_{c2} = Gr_{c1}\beta^2h^3n^2m^2,$$
$$M_1^2 = M^2smh^2, \sigma_1^2 = \sigma h^2, Br = \frac{\mu_1\upsilon^2}{\Delta Th_1^2k_1},$$
$$\Pr = \frac{\rho_1cp\upsilon_1}{k_1}, Br_1 = \frac{Br}{m^3n^2kh^2}, \Pr_1 = \frac{\Pr}{km}, Sc = \frac{D}{\upsilon},$$
$$Sr = \frac{Dk_T\Delta T}{T\Delta C}, K_1 = \frac{\gamma_1h_1^2}{\upsilon_1}, K_2 = K_1h^2mn$$

The non dimensional equations after dropping "asterisks" and for the feasibility and simplicity we consider $x_1 = x, y_1 = y$ and $t_1 = t$ in the region - I and $x_2 = x, y_2 = y, t_2 = t$ in the region -II.

$$\frac{\partial u_1}{\partial t} + u_1\frac{\partial u_1}{\partial x} + v_1\frac{\partial u_1}{\partial y} = -\frac{\partial p_1}{\partial x} + \left(\frac{\partial^2 u_1}{\partial x^2} + \frac{\partial^2 u_1}{\partial y^2}\right)$$
$$-\frac{1}{a^2}\left(\frac{\partial^2}{\partial x^2} + \frac{\partial^2}{\partial y^2}\right)^2 u_1 - \left(\sigma_1^2 + M^2\right)u_1 \tag{14}$$
$$+Gr_tT_1 + Gr_cC_1$$

$$\frac{\partial v_1}{\partial t} + u_1\frac{\partial v_1}{\partial x} + v_1\frac{\partial v_1}{\partial y} = -\frac{\partial p_1}{\partial y} + \left(\frac{\partial^2 v_1}{\partial x^2} + \frac{\partial^2 v_1}{\partial y^2}\right)$$
$$-\frac{1}{a^2}\left(\frac{\partial^2}{\partial x^2} + \frac{\partial^2}{\partial y^2}\right)^2 v_1 - \sigma_1^2 v_1 \tag{15}$$

$$\Pr\left(\frac{\partial T_1}{\partial t} + u_1\frac{\partial T_1}{\partial x} + v_1\frac{\partial T_1}{\partial y}\right) = \left(\frac{\partial^2 T_1}{\partial x^2} + \frac{\partial^2 T_1}{\partial y^2}\right)$$
$$+Br\left\{2\left[\left(\frac{\partial u_1}{\partial x}\right)^2 + \left(\frac{\partial v_1}{\partial y}\right)^2\right] + \left(\frac{\partial u_1}{\partial y} + \frac{\partial v_1}{\partial x}\right)^2\right\}$$
$$+\frac{Br}{a^2}\left[\left(\frac{\partial^2 v_1}{\partial x^2} + \frac{\partial^2 v_1}{\partial y^2}\right)^2 + \left(\frac{\partial^2 u_1}{\partial x^2} + \frac{\partial^2 u_1}{\partial y^2}\right)^2\right] \tag{16}$$
$$+QT_1 + \frac{4}{3}\frac{Rd}{k_1}\frac{\partial^2 T_1}{\partial y^2}$$

$$\frac{\partial C_1}{\partial t} + u_1\frac{\partial C_1}{\partial x} + v_1\frac{\partial C_1}{\partial y} = \frac{1}{Sc}\left(\frac{\partial^2 C_1}{\partial x^2} + \frac{\partial^2 C_1}{\partial y^2}\right)$$
$$+Sc_r\left(\frac{\partial^2 T_1}{\partial x^2} + \frac{\partial^2 T_1}{\partial y^2}\right) - K_1C_1 \tag{17}$$

Region –II

$$\frac{\partial u_2}{\partial t} + u_2\frac{\partial u_2}{\partial x} + v_2\frac{\partial u_2}{\partial y} = -\frac{\partial p_2}{\partial x} + \left(\frac{\partial^2 u_2}{\partial x^2} + \frac{\partial^2 u_2}{\partial y^2}\right)$$
$$-\left(\sigma_2^2 + M_2^2\right)u_2 + Gr_{t1}T_2 + Gr_{c1}C_2 \tag{18}$$

$$\frac{\partial v_2}{\partial t} + u_2\frac{\partial v_2}{\partial x} + v_2\frac{\partial v_2}{\partial y} = -\frac{\partial p_2}{\partial y} + \left(\frac{\partial^2 v_2}{\partial x^2} + \frac{\partial^2 v_2}{\partial y^2}\right)$$
$$-\frac{1}{a^2}\left(\frac{\partial^2}{\partial x^2} + \frac{\partial^2}{\partial y^2}\right)^2 v_2 - \sigma_2^2 v_2 \tag{19}$$

$$\Pr_1\left(\frac{\partial T_2}{\partial t} + u_2\frac{\partial T_2}{\partial x} + v_2\frac{\partial T_2}{\partial y}\right) = \left(\frac{\partial^2 T_2}{\partial x^2} + \frac{\partial^2 T_2}{\partial y^2}\right)$$
$$+Br_1\left\{2\left[\left(\frac{\partial u_2}{\partial x}\right)^2 + \left(\frac{\partial v_2}{\partial y}\right)^2\right] + \left(\frac{\partial u_2}{\partial y} + \frac{\partial v_2}{\partial x}\right)^2\right\} \tag{20}$$
$$+Q_1T_2 + \frac{4}{3}\frac{Rd}{kk_1}\frac{\partial^2 T_2}{\partial y^2}$$

$$\frac{\partial C_2}{\partial t} + u_2\frac{\partial C_2}{\partial x} + v_2\frac{\partial C_2}{\partial y} = \frac{Dmn}{Sc}\left(\frac{\partial^2 C_2}{\partial x^2} + \frac{\partial^2 C_2}{\partial y^2}\right)$$
$$+Dmn\,Sc_r\left(\frac{\partial^2 T_2}{\partial x^2} + \frac{\partial^2 T_2}{\partial y^2}\right) - K_2C_2 \tag{21}$$

Nondimensional boundary and interface conditions of velocity, temperature and concentration are

$$u_1 = v_1 = 0, \quad y = -1 + \varepsilon \cos(\lambda x + \theta)$$

$$\frac{\partial^2 u_1}{\partial y^2} = 0, \; y = -1 + \varepsilon \cos(\lambda x + \theta),$$

$$T_1 = 0, \quad y = -1 + \varepsilon \cos(\lambda x + \theta),$$

$$C_1 = 0, \quad y = -1 + \varepsilon \cos(\lambda x + \theta),$$

$$u_2 = v_2 = 0, \quad y = 1 + \frac{\varepsilon}{h}\cos(\lambda x)$$

$$T_2 = 1, \quad y = 1 + \frac{\varepsilon}{h}\cos(\lambda x)$$

$$C_2 = 1, \quad y = 1 + \frac{\varepsilon}{h}\cos(\lambda x)$$

$$u_1 = u_2, \; v_1 = v_2, \quad y = 0,$$

$$\left(\frac{\partial u_1}{\partial y} + \frac{\partial v_1}{\partial x}\right) - \frac{1}{a^2}\left(\frac{\partial^3 u_1}{\partial y^3} + \frac{\partial^3 v_1}{\partial x^3}\right) = \frac{1}{m^2 h^2 n}\left(\frac{\partial u_2}{\partial y} + \frac{\partial v_2}{\partial x}\right), \quad y = 0, \tag{22}$$

$$\frac{\partial p_1}{\partial x} = \frac{1}{nm^2 h^3}\frac{\partial p_2}{\partial x}, \quad y = 0$$

$$\frac{\partial^2 u_1}{\partial y^2} = 0, \; y = 0,$$

$$T_1 = T_2, \quad y = 0,$$

$$\left(\frac{\partial T_1}{\partial y} + \frac{\partial T_1}{\partial x}\right) = \frac{k}{h}\left(\frac{\partial T_2}{\partial y} + \frac{\partial T_2}{\partial x}\right), \quad y = 0$$

$$C_1 = C_2, \quad y = 0,$$

$$\left(\frac{\partial C_1}{\partial y} + \frac{\partial C_1}{\partial x}\right) = \frac{D}{h}\left(\frac{\partial C_2}{\partial y} + \frac{\partial C_2}{\partial x}\right), \quad y = 0$$

In the static fluid [3,6]:

$$-\frac{\partial p_1}{\partial x} - \frac{p_s g h_1^3}{\rho \nu_1^2} = -\frac{\partial p_2}{\partial x} - \frac{p_s g h_2^3}{\rho \nu_2^2} \tag{23}$$

where p_s is the static pressure, using Eq.(23) Eq.(14) and Eq.(18) will become

$$\frac{\partial u_1}{\partial t} + u_1\frac{\partial u_1}{\partial x} + v_1\frac{\partial u_1}{\partial y} = -\frac{\partial(p_1 - p_s)}{\partial x} + \left(\frac{\partial^2 u_1}{\partial x^2} + \frac{\partial^2 u_1}{\partial y^2}\right) - \frac{1}{a^2}\left(\frac{\partial^2}{\partial x^2} + \frac{\partial^2}{\partial y^2}\right)^2 u_1 - \left(\sigma_1^2 + M^2\right)u_1 + Gr_t T + Gr_c C_1 \tag{24}$$

$$\frac{\partial u_2}{\partial t} + u_2\frac{\partial u_2}{\partial x} + v_2\frac{\partial u_2}{\partial y} = -\frac{\partial(p_2 - p_s)}{\partial x} + \left(\frac{\partial^2 u_2}{\partial x^2} + \frac{\partial^2 u_2}{\partial y^2}\right) - \left(\sigma_2^2 + M_2^2\right)u_2 + Gr_{t1}T_2 + Gr_{c1}C_2 \tag{25}$$

Velocity, heat and mass distributions can be obtained by assuming

$$\begin{aligned} \boldsymbol{u}_1 &= \boldsymbol{u}_{10} + \boldsymbol{\varepsilon} e^{i(\lambda x + wt)}\boldsymbol{u}_{11} \\ \boldsymbol{v}_1 &= \boldsymbol{\varepsilon} e^{i(\lambda x + wt)}\boldsymbol{v}_{11} \\ \boldsymbol{T}_1 &= \boldsymbol{T}_{10} + \boldsymbol{\varepsilon} e^{i(\lambda x + wt)}\boldsymbol{T}_{11} \\ \boldsymbol{C}_1 &= \boldsymbol{C}_{10} + \boldsymbol{\varepsilon} e^{i(\lambda x + wt)}\boldsymbol{C}_{11} \\ \boldsymbol{u}_2 &= \boldsymbol{u}_{20} + \boldsymbol{\varepsilon} e^{i(\lambda x + wt)}\boldsymbol{u}_{21} \\ \boldsymbol{v}_2 &= \boldsymbol{\varepsilon} e^{i(\lambda x + wt)}\boldsymbol{v}_{21} \\ \boldsymbol{T}_2 &= \boldsymbol{T}_{20} + \boldsymbol{\varepsilon} e^{i(\lambda x + wt)}\boldsymbol{T}_{21} \\ \boldsymbol{C}_1 &= \boldsymbol{C}_{20} + \boldsymbol{\varepsilon} e^{i(\lambda x + wt)}\boldsymbol{C}_{21} \end{aligned} \tag{26}$$

Zeroth and first order equations obtained by subsituting the Eq. (26) in the Eq.(14) – Eq.(21) are given by

Region –I

$$\left(\frac{\partial^2 u_{10}}{\partial y^2}\right) - \frac{1}{a^2}\frac{\partial^4 u_{10}}{\partial y^4} - \left(\sigma_1^2 + M^2\right)u_{10} + Gr_t T_{10} + Gr_c C_{10} = 0 \tag{27}$$

$$\frac{\partial^2 T_{10}}{\partial y^2} + Br\left\{\left(\frac{\partial u_{10}}{\partial y}\right)^2\right\} + \frac{Br}{a^2}\left[\left(\frac{\partial^2 u_{10}}{\partial y^2}\right)^2\right] + QT_{10} + \frac{4}{3}\frac{Rd}{k_1}\frac{\partial^2 T_{10}}{\partial y^2} = 0 \tag{28}$$

$$\frac{1}{Sc}\left(\frac{\partial^2 C_{10}}{\partial y^2}\right) + Sc_r\left(\frac{\partial^2 T_{10}}{\partial y^2}\right) - K_1 C_{10} = 0 \tag{29}$$

$$\frac{\partial u_{11}}{\partial t} + (u_{10})\frac{\partial u_{11}}{\partial x} + (v_{11})\frac{\partial (u_{10})}{\partial y} = -\frac{\partial(p_{11} - p_s)}{\partial x} + \left(\frac{\partial^2 u_{11}}{\partial x^2} + \frac{\partial^2 u_{11}}{\partial y^2}\right) - \frac{1}{a^2}\left(\frac{\partial^2}{\partial x^2} + \frac{\partial^2}{\partial y^2}\right)^2 u_{11} - \left(\sigma_1^2 + M^2\right)u_{11} + Gr_t T_{11} + Gr_c C_{11} \tag{30}$$

$$\frac{\partial v_{11}}{\partial t}+u_{10}\frac{\partial v_{11}}{\partial x}=-\frac{\partial p_{11}-p_s}{\partial y}+\left(\frac{\partial^2 v_{11}}{\partial x^2}+\frac{\partial^2 v_{11}}{\partial y^2}\right)$$
$$-\frac{1}{a^2}\left(\frac{\partial^2}{\partial x^2}+\frac{\partial^2}{\partial y^2}\right)^2 v_{11}-\sigma_1{}^2 v_{11} \quad (31)$$

$$\Pr\left(\frac{\partial T_{11}}{\partial t}+u_{10}\frac{\partial T_{11}}{\partial x}+v_{11}\frac{\partial T_{11}}{\partial y}\right)=\left(\frac{\partial^2 T_{11}}{\partial x^2}+\frac{\partial^2 T_{11}}{\partial y^2}\right)$$
$$+Br\left\{2\left[\left(\frac{\partial u_{11}}{\partial x}\right)^2+\left(\frac{\partial v_{11}}{\partial y}\right)^2\right]+\left(\frac{\partial u_{11}}{\partial y}+\frac{\partial v_{11}}{\partial x}\right)^2\right\} \quad (32)$$
$$+\frac{Br}{a^2}\left[\left(\frac{\partial^2 u_{11}}{\partial x^2}+\frac{\partial^2 u_{11}}{\partial y^2}\right)^2\right]+QT_{11}+\frac{4}{3}\frac{Rd}{k_1}\frac{\partial^2 T_{11}}{\partial y^2}$$

$$\frac{\partial C_{11}}{\partial t}+u_{10}\frac{\partial C_{11}}{\partial x}+v_{11}\frac{\partial C_{11}}{\partial y}=\frac{1}{Sc}\left(\frac{\partial^2 C_{11}}{\partial x^2}+\frac{\partial^2 C_{11}}{\partial y^2}\right)$$
$$+Sc_r\left(\frac{\partial^2 T_{11}}{\partial x^2}+\frac{\partial^2 T_{11}}{\partial y^2}\right)-K_1 C_{11} \quad (33)$$

Region –II

$$\left(\frac{\partial^2 u_{20}}{\partial y^2}\right)-\left(\sigma_2{}^2+M_2{}^2\right)u_{20}+Gr_{t1}T_{20}+Gr_{c1}C_{20}=0 \quad (34)$$

$$\left(\frac{\partial^2 T_{20}}{\partial y^2}\right)+Br_1\left(\frac{\partial u_{20}}{\partial y}\right)^2+Q_1T_{20}+\frac{4}{3}\frac{Rd}{kk_1}\frac{\partial^2 T_{20}}{\partial y^2}=0 \quad (35)$$

$$\frac{Dmn}{Sc}\left(\frac{\partial^2 C_{20}}{\partial y^2}\right)+Dmn\,Sc_r\left(\frac{\partial^2 T_{20}}{\partial y^2}\right)-K_2C_{20}=0 \quad (36)$$

$$\frac{\partial u_{21}}{\partial t}+u_{20}\frac{\partial u_{21}}{\partial x}+v_{21}\frac{\partial u_{20}}{\partial y}=-\frac{\partial p_2}{\partial x}+\left(\frac{\partial^2 u_{21}}{\partial x^2}+\frac{\partial^2 u_{21}}{\partial y^2}\right)$$
$$-\left(\sigma_2{}^2+M_2{}^2\right)u_{21}+Gr_{t1}T_{21}+Gr_{c1}C_{21} \quad (37)$$

$$\frac{\partial v_{21}}{\partial t}+u_{20}\frac{\partial v_{21}}{\partial x}=-\frac{\partial p_2}{\partial y}+\left(\frac{\partial^2 v_{21}}{\partial x^2}+\frac{\partial^2 v_{21}}{\partial y^2}\right)$$
$$-\sigma_2{}^2 v_{21} \quad (38)$$

$$\Pr_1\left(\frac{\partial T_{21}}{\partial t}+u_{20}\frac{\partial T_{21}}{\partial x}+v_{21}\frac{\partial T_{20}}{\partial y}\right)=\left(\frac{\partial^2 T_{21}}{\partial x^2}+\frac{\partial^2 T_{21}}{\partial y^2}\right)$$
$$+Br_1\left\{2\left[\left(\frac{\partial u_{21}}{\partial x}\right)^2+\left(\frac{\partial v_{21}}{\partial y}\right)^2\right]+\left(\frac{\partial u_{21}}{\partial y}\frac{\partial v_{21}}{\partial x}\right)^2\right\} \quad (39)$$
$$+Q_1T_{21}+\frac{4}{3}\frac{Rd}{kk_1}\frac{\partial^2 T_{21}}{\partial y^2}$$

$$\frac{\partial C_{21}}{\partial t}+u_{20}\frac{\partial C_{21}}{\partial x}+v_{21}\frac{\partial C_{20}}{\partial y}=\frac{Dmn}{Sc}\left(\frac{\partial^2 C_{21}}{\partial x^2}+\frac{\partial^2 C_{21}}{\partial y^2}\right)$$
$$+Dmn\,Sc_r\left(\frac{\partial^2 T_{21}}{\partial x^2}+\frac{\partial^2 T_{21}}{\partial y^2}\right)-K_2C_{21} \quad (40)$$

The solutions of zeroth order eqautions can be obtained by using the following boundary conditions.

$$u_{10}=0,\quad y=-1,$$
$$u_{11}=-e^{(\lambda x+\theta)}u_{10}{}',\quad y=-1$$
$$\frac{\partial^2 u_{10}}{\partial y^2}=0,\quad y=-1,$$
$$\frac{\partial^2 u_{11}}{\partial y^2}=-e^{(\lambda x+\theta)}u_{10}{}''$$
$$T_{10}=0,\quad y=-1$$
$$T_{11}=-e^{(\lambda x+\theta)}T_{10}{}',\quad y=-1$$
$$C_{10}=0,\quad y=-1,$$
$$C_{11}=-e^{(\lambda x+\theta)}C_{10}{}',y=-1 \quad (41)$$
$$u_{20}=0,\quad y=1,$$
$$u_{21}=-\frac{e^{(\lambda x)}}{h}u_{20}{}',\quad y=1$$
$$T_{20}=1,\quad y=1,$$
$$T_{21}=-\frac{e^{(\lambda x)}}{h}T_{20}{}',\quad y=1$$
$$C_{20}=1,\quad y=1,$$
$$C_{21}=-\frac{e^{(\lambda x)}}{h}C_{20}{}',\quad y=1$$

$$u_{10}=u_{20},\quad y=0,$$
$$u_{11}=u_{21},\quad y=0,$$
$$v_{11}=v_{21},\quad y=0,$$
$$\frac{\partial u_{10}}{\partial y}-\frac{1}{a^2}\frac{\partial^3 u_{10}}{\partial y^3}=\frac{1}{m^2h^2n}\frac{\partial u_{20}}{\partial y},$$
$$\left(\frac{\partial u_{11}}{\partial y}+\frac{\partial v_{11}}{\partial x}\right)-\frac{1}{a^2}\left(\frac{\partial^3 u_{11}}{\partial y^3}+\frac{\partial^3 v_{11}}{\partial x^3}\right)$$
$$=\frac{1}{m^2h^2n}\left(\frac{\partial u_{21}}{\partial y}+\frac{\partial v_{21}}{\partial x}\right),\quad y=0,$$

$$\frac{\partial^2 u_{10}}{\partial y^2}=0,\quad y=0,$$

$$\frac{\partial^2 u_{11}}{\partial y^2}=0,\quad =0,$$

$$\frac{\partial p_1}{\partial x}=\frac{1}{nm^2h^3}\frac{\partial p_2}{\partial x},\quad y=0,$$

$$T_{10}=T_{20},\quad y=0,$$

$$T_{11}=T_{21},\quad y=0,$$

$$\frac{\partial T_{10}}{\partial y}=\frac{k}{h}\frac{\partial T_{20}}{\partial y},\quad y=0,$$

$$\left(\frac{\partial T_{11}}{\partial y}\right)=\frac{k}{h}\left(\frac{\partial T_{21}}{\partial y}\right),\quad y=0,$$

$$C_{10}=C_{20},\quad y=0,$$

$$C_{11}=C_{21},\quad y=0,$$

$$\frac{\partial C_{10}}{\partial y}=\frac{D}{h}\frac{\partial C_{20}}{\partial y},\quad y=0,$$

$$\left(\frac{\partial C_{11}}{\partial y}\right)=\frac{D}{h}\left(\frac{\partial C_{21}}{\partial y}\right),\quad y=0$$

In order to solve first order equations stream functions are introduced which is used to reduce the dependent variables and also eliminate the pressure from the list of the variables.

$$\begin{aligned} u_{11}&=-\frac{\partial \psi_1}{\partial y}, \qquad v_{11}=\frac{\partial \psi_1}{\partial x}\\ u_{21}&=-\frac{\partial \psi_2}{\partial y}, \qquad v_{21}=\frac{\partial \psi_2}{\partial x} \end{aligned} \tag{42}$$

where

$$\begin{aligned} \psi_1&=e^{i(\lambda x+\omega t)}\psi_1\\ \psi_2&=e^{i(\lambda x+\omega t)}\psi_2\\ T_{11}&=e^{i(\lambda x+\omega t)}T_{11}\\ T_{21}&=e^{i(\lambda x+\omega t)}T_{21}\\ C_{11}&=e^{i(\lambda x+\omega t)}C_{11}\\ C_{21}&=e^{i(\lambda x+\omega t)}C_{21} \end{aligned} \tag{43}$$

by substituting Eq.(42) and Eq.(43) in Eq.(30)-Eq.(33) and Eq.(37)-Eq.(40), we have

$$\begin{aligned} i\omega\frac{\partial^2\psi_1}{\partial y^2}&=\frac{\partial^4\psi_1}{\partial y^4}-\left(\sigma^2+M^2\right)\frac{\partial^2\psi_1}{\partial y^2}-\frac{1}{a^2}\frac{\partial^6\psi_1}{\partial y^6}\\ &-Gr_t\frac{\partial T_{11}}{\partial y}-Gr_c\frac{\partial C_{11}}{\partial y} \end{aligned} \tag{44}$$

$$\begin{aligned} i\omega\,\mathrm{Pr}\,T_{11}&=\frac{\partial^2 T_{11}}{\partial y^2}+Br\left(\frac{\partial^2\psi_1}{\partial y^2}\right)^2+\frac{Br}{a^2}\left(\frac{\partial^3\psi_1}{\partial y^3}\right)^2\\ &+Q_1T_{11}+\frac{4Rd}{3k_1}\frac{\partial^2 T_{11}}{\partial y^2} \end{aligned} \tag{45}$$

$$i\omega Sc\,C_{11}=\frac{\partial^2 C_{11}}{\partial y^2}+Sc\,Sc_r\frac{\partial^2 T_{11}}{\partial y^2}-K_1C_{11} \tag{46}$$

$$\begin{aligned} i\omega\frac{\partial^2\psi_2}{\partial y^2}&=\frac{\partial^4\psi_2}{\partial y^4}-\left(\sigma_1^2+M_1^2\right)\frac{\partial^2\psi_1}{\partial y^2}\\ &-Gr_{t1}\frac{\partial T_{21}}{\partial y}-Gr_{c1}\frac{\partial C_{21}}{\partial y} \end{aligned} \tag{47}$$

$$\begin{aligned} i\omega\,\mathrm{Pr}_1T_{21}&=\frac{\partial^2 T_{21}}{\partial y^2}+Br_1\left(\frac{\partial^2\psi_2}{\partial y^2}\right)^2+Q_1T_{21}\\ &+\frac{4Rd}{3kk_1}\frac{\partial^2 T_{21}}{\partial y^2} \end{aligned} \tag{48}$$

$$\begin{aligned} i\omega ScC_{21}&=D\,m\,n\frac{\partial^2 C_{21}}{\partial y^2}+D\,m\,n\,Sc\,Sc_r\frac{\partial^2 T_{21}}{\partial y^2}\\ &-K_2C_{21} \end{aligned} \tag{49}$$

with the boundary conditions

$$\left.\begin{aligned} &\frac{\partial\psi_1}{\partial y}=e^{i(\theta-\omega t)}u_{10}',\\ &\frac{\partial^3\psi_1}{\partial y^3}=e^{i(\theta-\omega t)}u_{10}'',\\ &T_{10}=0,\\ &C_{10}=0,\\ &C_{11}=-e^{(\lambda x+\theta)}C_{10}',\\ &T_{11}=-e^{(\lambda x+\theta)}T_{10}' \end{aligned}\right\}_{y=-1} \tag{50}$$

$$\left.\begin{aligned} &\frac{\partial\psi_2}{\partial y}=e^{i(-\omega t)}u_{20}',\\ &T_{20}=1,\\ &T_{21}=-e^{(\lambda x)}T_{20}',\\ &C_{20}=1,\\ &C_{21}=-e^{(\lambda x)}C_{20}', \end{aligned}\right\}_{y=1}$$

$$\left.\begin{aligned}&\frac{\partial \psi_1}{\partial y}=\frac{\partial \psi_2}{\partial y},\\&\psi_1=\psi_2,\\&\frac{\partial^2 \psi_1}{\partial y^2}-\frac{1}{a^2}\frac{\partial^4 \psi_1}{\partial y^4}=\frac{1}{nm^2h^2}\frac{\partial^2 \psi_2}{\partial y^2},\\&\frac{\partial^3 \psi_1}{\partial y^3}=0,\end{aligned}\right\}_{y=0}$$

$$\begin{aligned}&i\omega\frac{\partial^2 \psi_1}{\partial y^2}-\frac{\partial^4 \psi_1}{\partial y^4}+\left(\sigma^2+M^2\right)\frac{\partial^2 \psi_1}{\partial y^2}\\&+\frac{1}{a^2}\frac{\partial^6 \psi_1}{\partial y^6}+Gr_t\frac{\partial T_{11}}{\partial y}+Gr_c\frac{\partial C_{11}}{\partial y}\\&=\frac{1}{nm^2h^3}\left(\begin{aligned}&i\omega\frac{\partial^2 \psi_2}{\partial y^2}-\frac{\partial^4 \psi_2}{\partial y^4}+\left({\sigma_1}^2+{M_1}^2\right)\frac{\partial^2 \psi_1}{\partial y^2}\\&+Gr_{t1}\frac{\partial T_{21}}{\partial y}+Gr_{c1}\frac{\partial C_{21}}{\partial y}\end{aligned}\right)_{y=0}\end{aligned}$$

$$\left.\begin{aligned}&C_{10}=C_{20},\\&C_{11}=C_{21},\\&\frac{\partial C_{10}}{\partial y}=\frac{D}{h}\frac{\partial C_{20}}{\partial y},\\&\left(\frac{\partial C_{11}}{\partial y}\right)=\frac{D}{h}\left(\frac{\partial C_{21}}{\partial y}\right),\end{aligned}\right\}_{y=0}$$

$$\left.\begin{aligned}&T_{10}=T_{20},\\&T_{11}=T_{21},\\&\frac{\partial T_{10}}{\partial y}=\frac{k}{h}\frac{\partial T_{20}}{\partial y},\\&\left(\frac{\partial T_{11}}{\partial y}\right)=\frac{k}{h}\left(\frac{\partial T_{21}}{\partial y}\right)\end{aligned}\right\}_{y=0}$$

The equations for total velocity, temperature, and concentration are the sum of the mean and perturbed parts.

$$\begin{aligned}&u_1(y)=u_{10}(y)-\varepsilon\left(-\cos(\lambda x+\omega t)+\sin(\lambda x+\omega t)\right)\frac{\partial \psi_1}{\partial y}\\&T_1(y)=T_{10}(y)+\varepsilon\left(\cos(\lambda x+\omega t)-\sin(\lambda x+\omega t)\right)T_{11}(y)\\&C_1(y)=C_{10}(y)+\varepsilon\left(\cos(\lambda x+\omega t)-\sin(\lambda x+\omega t)\right)C_{11}(y)\end{aligned}$$

(51)

Both the mean part (zeroth order) Eq.(27)-Eq.(29) & Eq.(34)-Eq.(36) and the perturbed part (first order) Eq.(44)-Eq.(59) with the boundary conditions Eq.(50) are solved using NDSolve command in Mathematica software.

Non dimensional form of the shear stress is given by [3,5].

$$\tau=\left(\frac{h^2}{\rho\nu^2}\right)\tau_{xy}=\frac{\partial u}{\partial y}+\frac{\partial v}{\partial x} \tag{52}$$

At the wall $y=-1+\varepsilon\cos(\lambda x+\theta)$, shear stress is given by

$$\tau_1=u_{10}'(-1)+\mathrm{Re}\left[\varepsilon e^{i(\lambda x+\theta)}u_{10}''(-1)-\varepsilon e^{i(\lambda x+\omega t)}\psi_1'(-1)\right]$$

(53)

and at the wall $y=1+\varepsilon\cos(\lambda x)$ is given by

$$\tau_2=u_{20}'(1)+\mathrm{Re}\left[\varepsilon e^{i\lambda x}u_{20}''(1)-\varepsilon e^{i(\lambda x+\omega t)}\psi_2''(1)\right]$$

(54)

At the walls $y=-1+\varepsilon\cos(\lambda x+\theta)$ and $y=1+\varepsilon\cos(\lambda x)$ heat transfer is given by

$$Nu_1=T_{10}'(-1)+\mathrm{Re}\left[\varepsilon e^{i(\lambda x+\theta)}T_{10}''(-1)+\varepsilon e^{i(\lambda x+\omega t)}T_{11}'(-1)\right]$$

(55)

$$Nu_2=T_{20}'(1)+\mathrm{Re}\left[\varepsilon e^{i\lambda x}T_{20}''(1)+\varepsilon e^{i(\lambda x+\omega t)}T_{21}'(1)\right]$$

(56)

Sherwood Number at the walls is given by [3,5]

$$Sh_1=C_{10}'(-1)+\mathrm{Re}\left[\varepsilon e^{i(\lambda x+\theta)}C_{10}''(-1)+\varepsilon e^{i(\lambda x+\omega t)}C_{11}'(-1)\right]$$

(57)

$$Sh_2=C_{20}'(1)+\mathrm{Re}\left[\varepsilon e^{i\lambda x}C_{20}''(1)+\varepsilon e^{i(\lambda x+\omega t)}C_{21}'(1)\right]$$

(58)

Using the second law of thermodynamics the Entropy generation is given by

$$\begin{aligned}EG_0=&\frac{k_1}{T_0}\left(1+\frac{4Rd}{3k}\right)\left(\frac{\partial T_1}{\partial y}\right)^2+\frac{\mu_1}{T_0}\left[\left(\frac{\partial u_1}{\partial y}\right)^2+\left(\frac{\partial v_1}{\partial x}\right)^2+\left(\frac{\partial u_1}{\partial y}+\frac{\partial v_1}{\partial x}\right)^2\right]\\&+\frac{\eta}{T_0}\left(\frac{\partial^2 u}{\partial y^2}\right)^2+\frac{RD}{C_0}\left(\frac{\partial C_1}{\partial y}\right)^2+\frac{RD}{T_0}\left(\frac{\partial C_1}{\partial y}\right)\left(\frac{\partial T_1}{\partial y}\right)\end{aligned}$$

(59)

$$\begin{aligned}EG_2=&\frac{k_2}{T_0}\left(1+\frac{4Rd}{3k}\right)\left(\frac{\partial T_2}{\partial y}\right)^2+\frac{\mu_2}{T_0}\left[\left(\frac{\partial u_2}{\partial y}\right)^2+\left(\frac{\partial v_2}{\partial x}\right)^2+\left(\frac{\partial u_2}{\partial y}+\frac{\partial v_2}{\partial x}\right)^2\right]\\&+\frac{RD}{C_0}\left(\frac{\partial C_2}{\partial y}\right)^2+\frac{RD}{T_0}\left(\frac{\partial C_2}{\partial y}\right)\left(\frac{\partial T_2}{\partial y}\right)\end{aligned}$$

(60)

The non dimensional entropy generation is given by

$$\begin{aligned}EG_1(y)=&\left(1+\frac{4Rd}{3k_1}\right)\left(\frac{\partial T_1}{\partial y}\right)^2+\frac{Br}{\delta}\left(\frac{\partial u_1}{\partial y}\right)^2\\&+\frac{Br}{\delta a^2}\left(\frac{\partial^2 u_1}{\partial y^2}\right)^2+\frac{\xi L}{\delta}\left(\frac{\partial C_1}{\partial y}\right)+\frac{L}{\delta}\left(\frac{\partial C_1}{\partial y}\frac{\partial T_1}{\partial y}\right)\end{aligned} \tag{61}$$

$$EG_2(y)=\left(1+\frac{4Rd}{3k_1}\right)\left(\frac{\partial T_2}{\partial y}\right)^2+\frac{Br_1}{\delta}\left(\frac{\partial u_2}{\partial y}\right)^2 +\frac{\xi L}{\delta}\left(\frac{\partial C_2}{\partial y}\right)+\frac{L}{\delta}\left(\frac{\partial C_2}{\partial y}\frac{\partial T_2}{\partial y}\right) \quad (62)$$

Bejan number Be known as the ratio of entropy generation produced by heat and mass transfer to total entropy generation, is an alternative irreversibility distribution parameter and is given by

$$Be_1(y)=\frac{EG_{n_1}}{EG_1(y)}$$

$$Be_2(y)=\frac{EG_{n_2}}{EG_2(y)}$$

$$EG_{n_1}=\left(1+\frac{4Rd}{3k_1}\right)\left(\frac{\partial T_1}{\partial y}\right)^2+\frac{\xi L}{\delta}\left(\frac{\partial C_1}{\partial y}\right)+\frac{L}{\delta}\left(\frac{\partial C_1}{\partial y}\frac{\partial T_1}{\partial y}\right)$$

$$EG_{n_2}=\left(1+\frac{4Rd}{3k_1}\right)\left(\frac{\partial T_1}{\partial y}\right)^2+\frac{\xi L}{\delta}\left(\frac{\partial C_1}{\partial y}\right)+\frac{L}{\delta}\left(\frac{\partial C_1}{\partial y}\frac{\partial T_1}{\partial y}\right) \quad (63)$$

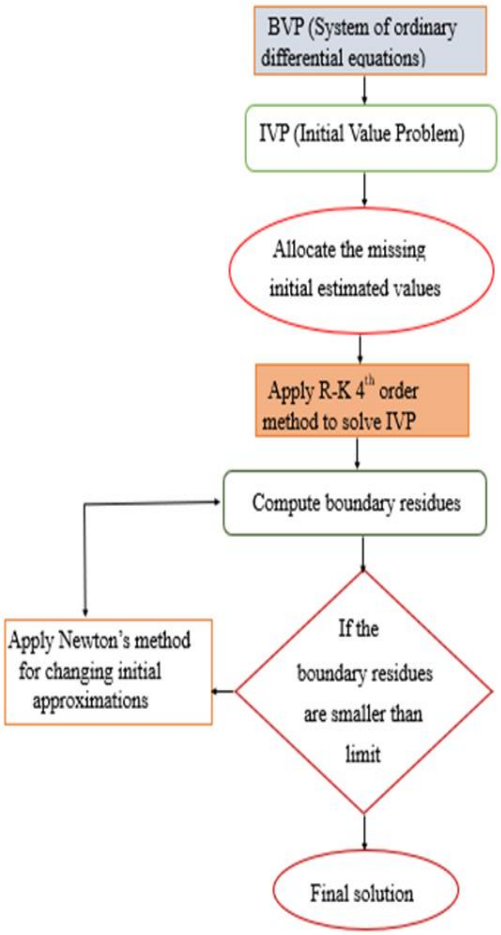

Fig. 2. Flow Chart of R-K Fourth Order method

4. Results and Discussion

The governing equations contain both a mean and a perturbed term. Using a long-wave approximation, the perturbed part is solved. Total velocity, temperature, and concentrations equal the sum of their mean and perturbed parts Eq.(51). The mean and perturbed parts of the governing equations are turned into coupled non-linear differential equations that are solved using the RK technique coupled with the shooting method by considering the NDSolve command in MATHEMATICA. Moreover, the working scheme of R-K fourth order can been seen Fig. 2. The obtained results are depicted graphically from Fig (3) to Fig (5) for various parameters. Due to the increase in the Hartmann number, we observe a decrease in velocity in Fig. 3(a). The application of a magnetic field in the direction normal to the flow field slows the fluid's motion and thus generates the Lortenz force in the opposite direction of the fluid flow. As seen in Fig. 3(b), increasing the porous parameter reduces the flow of the fluid; the effect of the porous parameter is to reduce the fluid velocity due to the Damping effect. Fig. 3(c) depicts the effect of Gr_ton fluid velocity; increasing the Gr_t values emphasizes fluid motion due to buoyancy force, resulting in a rise in velocity distribution. Variation of the velocity distribution is portrayed in Fig. 3(d) with a change in the couple- stress parameter. As the couple- stress parameter increases, we observe a rise in fluid movement in region-I, but no change in region-II. This is because, as as $\alpha \to \infty, \eta \to 0$, we obtain the case of a Newtonian fluid. The existence of heat generation produces thermal energy, raising the fluid's temperature. The fluid velocity escalates which is elucidated in Fig.3(e) as a result of the increasing thermal buoyancy force. From Fig. 3(f), one can observe that the fluid's velocity drops as the waviness (roughness) λ increases.

Fig 4(a)-(d) show the variations of the temperature distribution due to changes in the parameters Br, K_1, σ, and M.

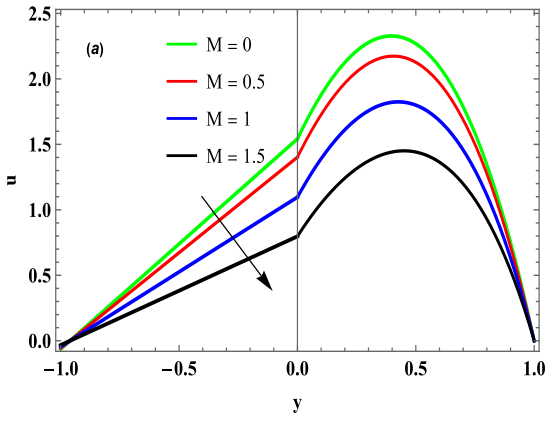

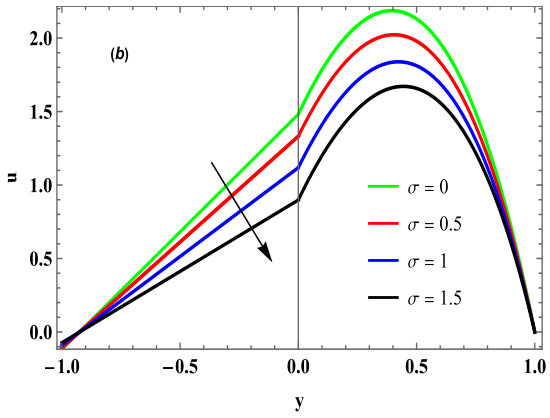

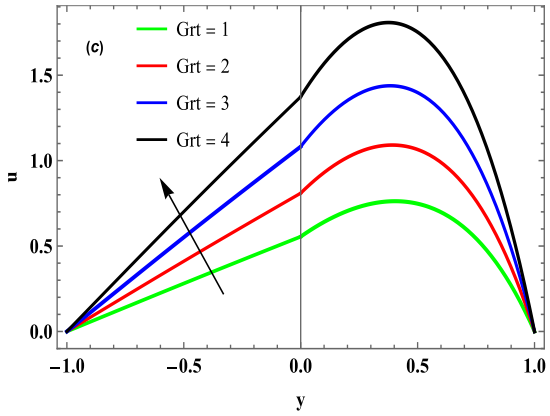

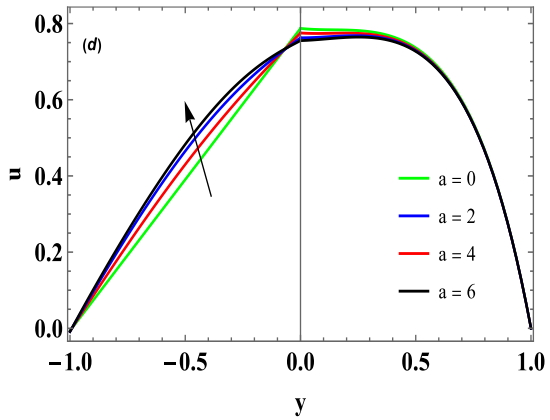

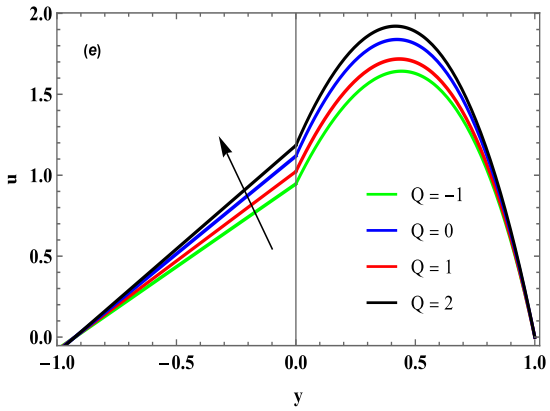

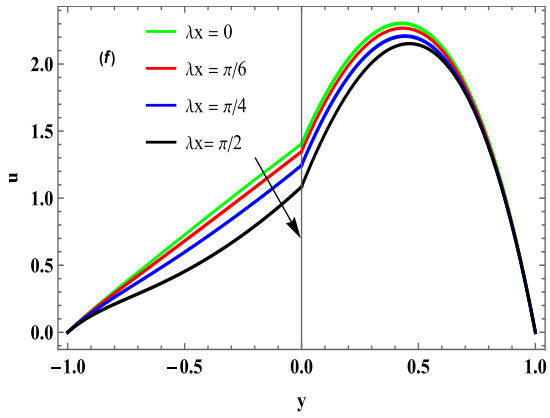

Fig. 3. Variation of Velocity distribution for $Pr = 0.71$, $Br = 0.5$, $s = 2$, $Gr_c = 2$, $Rd = 1$, $\lambda x = \pi/2$ by varying: (a) Hartmann number $Q = 1$;(b) porous parameter $n = 1, Gr_t = 1$, $Q = 1$; (c) Grasoff number $n = 1$, $M = 1$, $Q = 1$; (d) couple- stress parameter $n = 1.5$, $M = 1$, $Q = 1$; (e) heat generation and absorption parameter $n = 1.5$, $M = 1$; (f) wavy number $n = 1.5$, $M = 1$, $Q = 1$.

Raising the Br values causes the temperature to increase because they represent the coefficient of Joule and viscous dissipation, which can be seen in Fig. 4(a). The distribution of temperature has increased as a result of an increase in heat generation, as seen in Fig. 4(b).

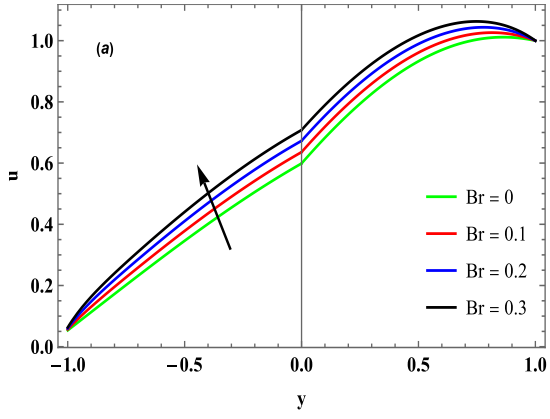

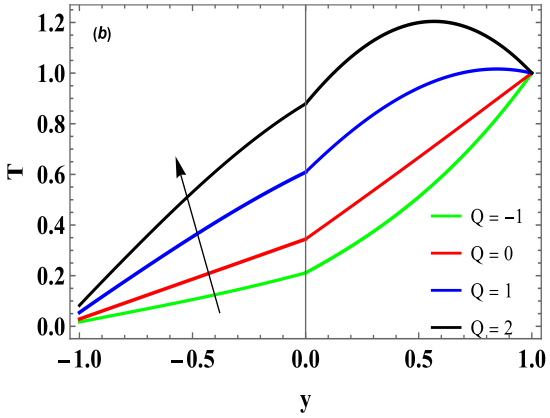

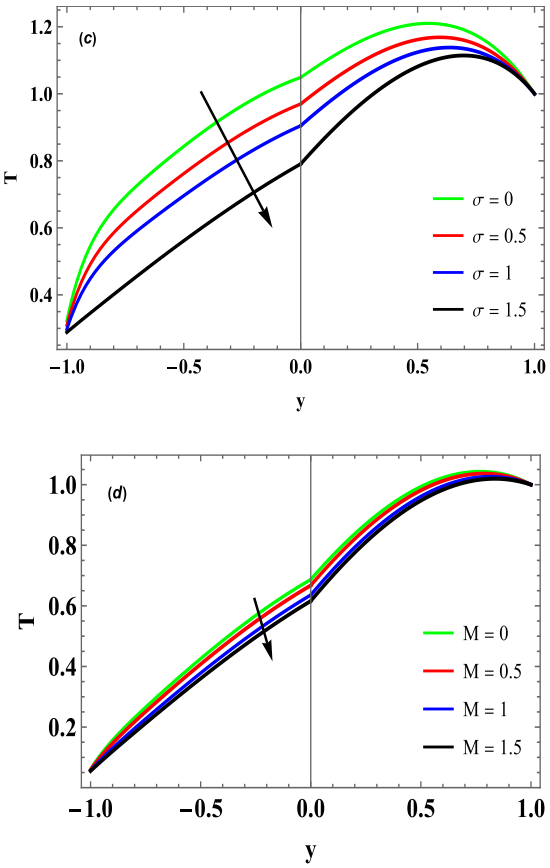

Fig. 4. Variation of Temperature distribution for $Pr = 0.71$, $Gr_c = 2$, $s = 2$, $Br = 0.5$, $n = 1.4$, $k = 1$, $m = 1.4$, $\sigma = 1$, $Rd = 1$, $\lambda x = \pi/2$ by varying: (a) Brikmann number M = 1, $Gr_t = 1$; (b) heat generation or absorption M = 1, $Gr_t = 1$; (c) the Porous parameter M = 1, $Gr_t = 1$; (d) Hartmann number Gr_t= 2.

The positive value of Q implies heat generation, while the negative sign denotes heat absorption. Heat generation physically indicates the production of heat, which raises the temperature in the flow field. We can see from Fig. 4(c) that the temperature drops as the porosity parameter increases. The primary cause of the temperature drop is the loss of specific heat and thermal conductivity due to the influence of porosity. As the Hartman number rises, we see that the temperature decreases which can be seen Fig. 4(d).

Fig. (5) shows how the concentration distribution varies when the parameters K_1, Sc, and Sr vary. Concentration reduces with first-order chemical reaction K_1, as shown in Fig. 5(a). Because higher K_1,values reduce chemical molecule diffusivity and reduce species concentration. As shown in Fig. 5(b) and 5(c), mass diffusion drops with the increase in the Schmidt and Soret number, resulting in a reduction of concentration.

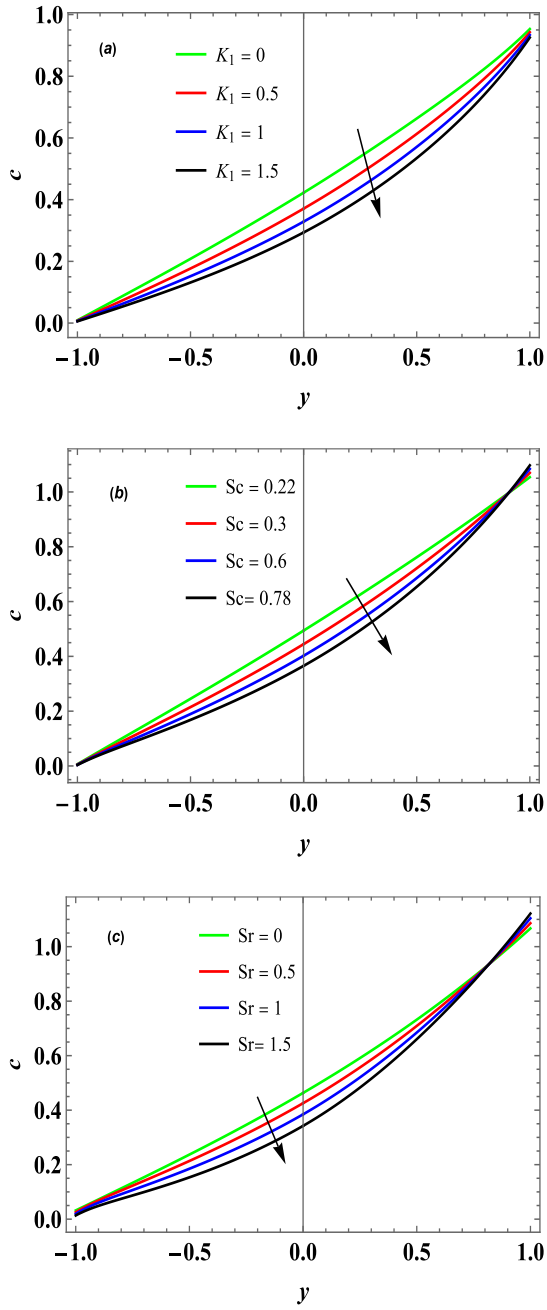

Fig. 5. Variation Concentration distribution for $Pr = 0.71$, $M = 1$, $Gr_t = 2$, $Gr_c = 2$, $Rd = 1$, $n = 1.5$, $D = 0.5$, $\lambda x = \pi/4$ by varying: (a) chemical reaction; (b) the Schmidt number $Sr = 0.5$; (c) Soret number $Sc = 0.5$.

The variation of Entropy generation with parameters Br, M, σ *and* K_1 is shown in Fig 6. Br and thermal conductivity have an inverse relationship. Fig. 6(a) illustrates that as Br increases, the thermal conductivity decreases and the rate of entropy generated rises. Due to Lorentz force, the increase in the Hartmann number disrupts the fluid flow, resulting in a decrease in temperature. As shown in Fig. 6(b), entropy decreases as a direct result of temperature. The rate of entropy generation falls as the porosity parameter rises in Fig. 6(c), because fluid velocity reduces the random motion of the fluid particles.

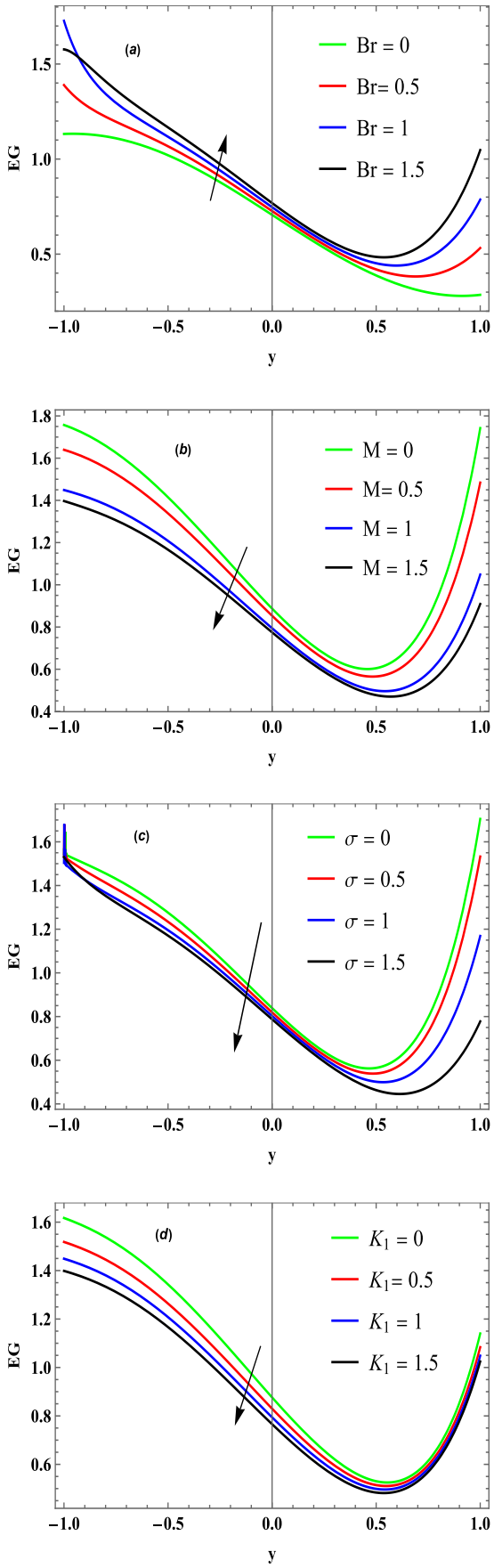

Fig. 6. Variation of Entropy generation for $n = 1.5$, $m = 1.4$, $Rd = 1$, $Gr_t = 5$, $Gr_c = 2$, $Q = 1$, $s = 2$, $Pr = 0.71$ by varying: (a) Brikaman number; (b) couple-stress number; (c) Hartmann number; (d) Porous Parameter

Figure 6(d) illustrates the impact of the chemical reaction parameter on the entropy generation. Enhancing the chemical reaction parameter results in a reduction of entropy production in the flow. Less entropy is produced when the fluid moves through the channel because the chemical bond-breaking process uses more kinetic energy.

The variation of the Bejan number by varying the Hartmann number, couple- stress fluid parameter, and porous parameter is presented in Figure 7. As shown in Fig. 7(a), when *Br* increases, the Bejan number exhibits inverse behaviour to that of entropy generation. Figure 7(b) demonstrates that when the Hartmann number rises, so does the Bejan number. The variations of the Bejan number illustrate the contribution of friction irreversibility to entropy generation thereby increasing as *M* is increased. As can be observed in Fig. 7(c), the Bejan number rises as the porosity parameter escalates. In Fig. 7(d), we can see that the Bejan number rises as the chemical reaction progresses.

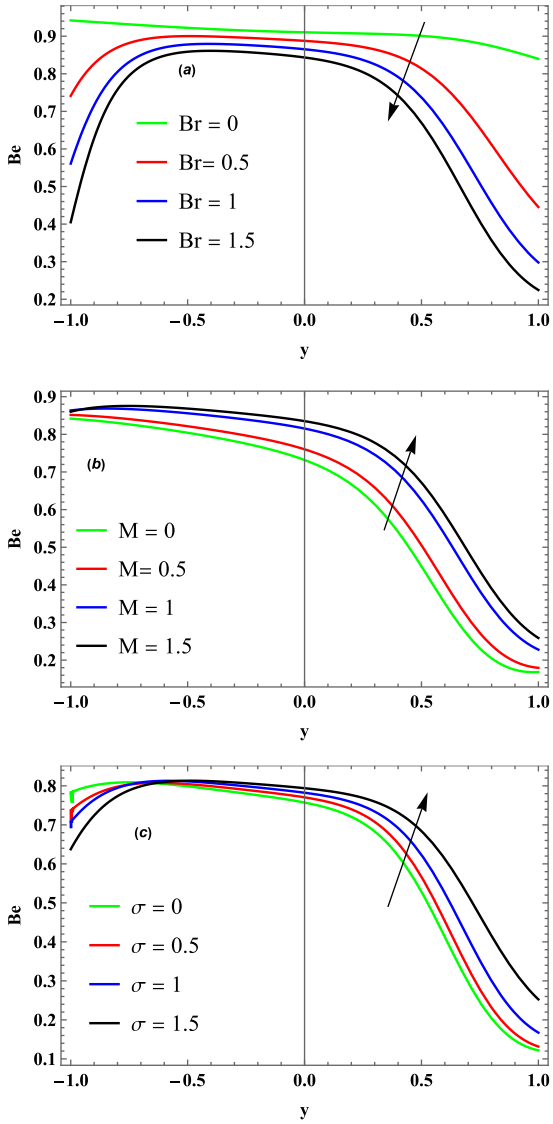

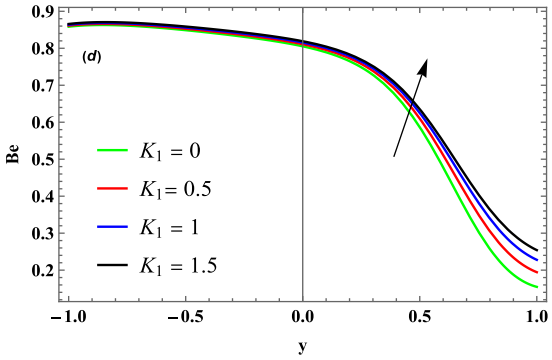

Fig. 7. Variation of Bejan number for $n = 1$, $m = 1$, $Rd = 1$, $Gr_t = 2$, $Gr_c = 2$, $Q = 1$, $s = 2$, $Pr = 0.71$, $Br = 0.5$ by varying: (a) Brikaman number; (b) couple-stress number M = 1, σ = 1; (c) Hartmann number; (d) porous Parameter M = 1.

Fig. 8 illustrates the variations of the Nusselt number at the walls caused with the influence of the parameters Q, M, and σ. Fig. 8(a) and 8(b) show that the Nusselt number grows at the left wall and drops at the right wall, respectively, as the heat generation and absorption increase. A negative Nusselt number indicates that heat is transmitted to the wall from the fluid. The figure shows that fluctuations in the local Nusselt number follow a wavy pattern. Physically, it is due to the modification of thermal boundary layer thickness caused by the wavy wall. Heat transfer reduces as the internal heat generation parameter increases.

When $Q < 0$, the heat transfer rate is high as the fluid in the cavity absorbs heat and immediately transfers it to the fluid from the wall, creating a positive gradient of heat transfer. On the other hand, when $Q > 0$, heat is generated in the fluid. absorbs less heat, and excess produced heat is transported to the wall from the fluid, resulting in a negative gradient of local heat transfer. Fig. 8(c) and Fig. 8(d) shows that when the Hartmann number grows, the Nusselt number drops at the left wall and rises at the right wall.

When the porosity parameter is raised, the Nusselt number drops at the left channel boundary and escalates at the right channel boundary, as shown in Figs. 8(e) and 8(f). This is due to the variation in temperature gradient at both the walls of the channel.

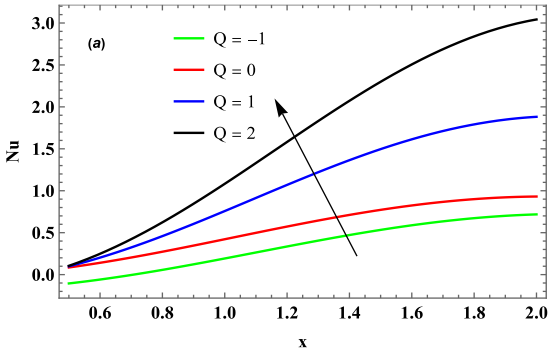

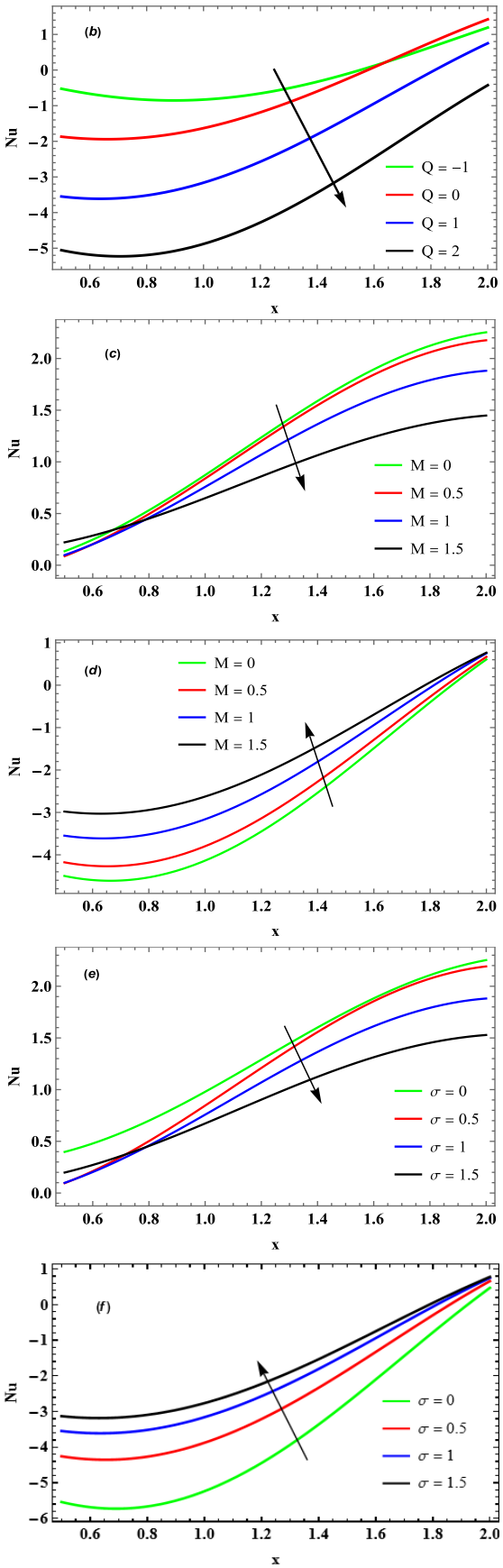

Fig. 8. Variation of Nusselt Number for Gr_t = 2, s = 2, σ = 1, Gr_c = 2, Pr = 0.71, Br = 0.5, n = 1.5, by varying: (a) heat generation and absorption at left wall; (b) heat generation and absorption at right wall M = 1; (c) Hartmann number at left wall; (d) Hartmann number at right wall Q = 1; (e) Porous parameter at left wall; (f) The porous parameter at right wall.

Fig. 9 exemplifies how the Sherwood number varies when the parameters K_1 , Sc, and Sr varied. Fig. 9(a) and 9(b) demonstrate this. that when the chemical reaction increases, the Sherwood number reduces on the left wall and rises on the right wall of the channel. Fig. 9(c) and 9(d) demonstrate that when the Sc increases, the Sherwood number decreases in the middle of the wave on the left wall and enhances at the right wall. When Sr increases, the Sherwood number rises at both the walls of the channel, as shown in Fig. 9(e) and (f).

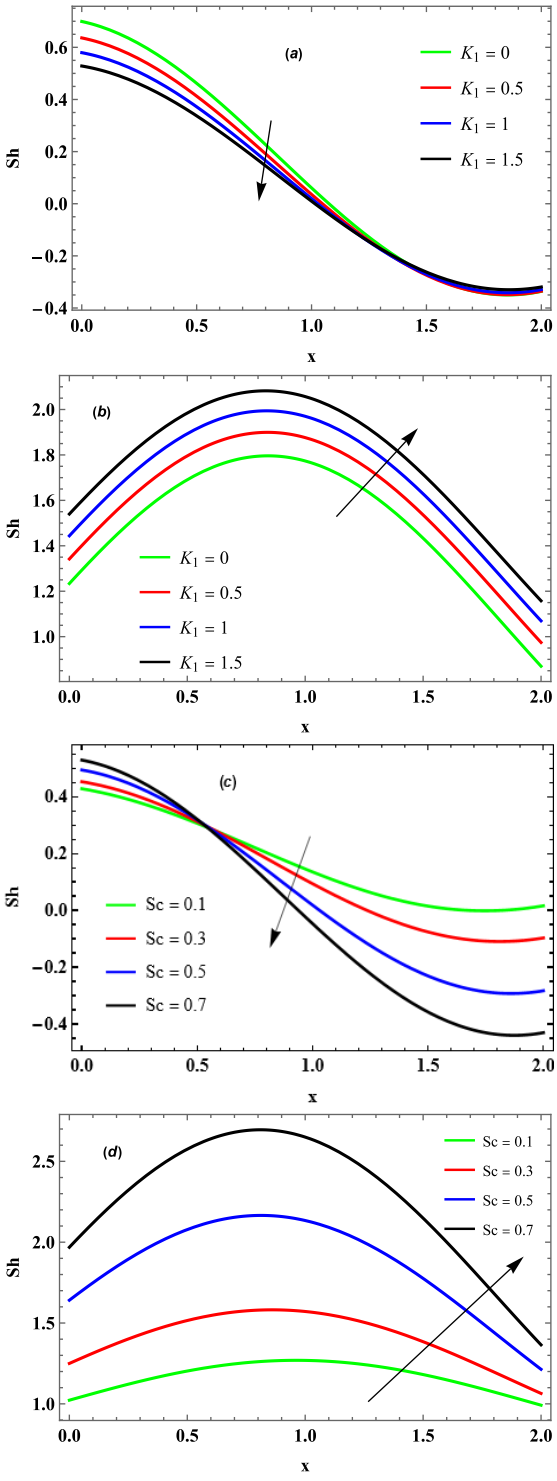

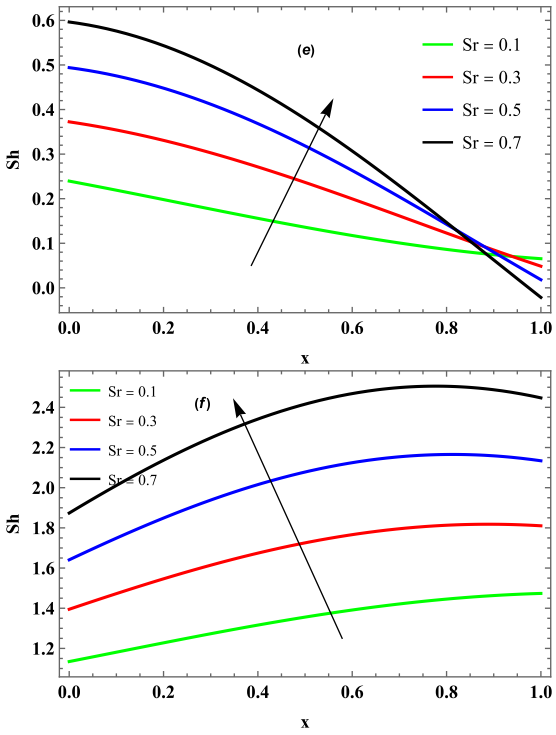

Fig. 9. Variation of Sherwood Number for n=1.4, M=1, Gr_t= 2, Gr_c = 2, Q = 1, s = 2, σ = 1, Pr = 0.71, Br = 0.5 by varying: (a) Chemical reaction at left wall; (b) Chemical reaction at right wall; (c) the Schmidt number at left wall; (d) The Schmidt number at right wall; (e) Soret number at left wall; (f) The Soret number at right wall.

Fig. 10 depicts the variance of shear stress on the channel walls. Fig. 10(a) reveals that when Gr_t increases, shear stress drops at the left wall and grows at the right wall. According to Fig. 10(b), when the Hartmann number M increases, the shear stress escalates at the left wall and falls at the right wall.

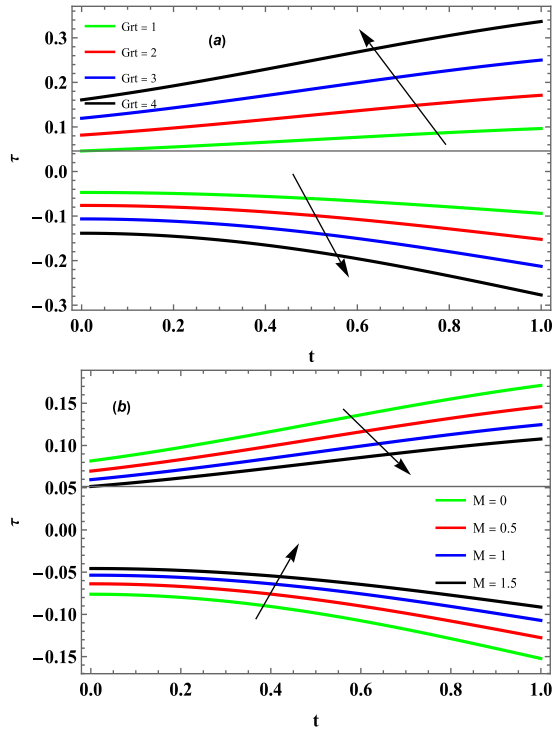

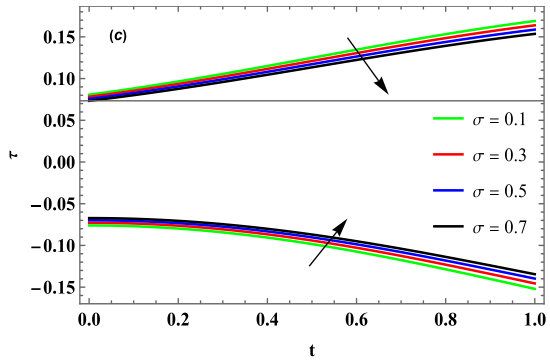

Fig. 10. Variation of Shear stress by varying: (a) Grashoff number; (b) Hartmann number n = 1.5, Grt = 2, Q = 1, s = 3, Pr = 0.71, Br = 0.5; (c) porous parameter

When the porous parameter is increased, shear stress rises at the left wall and drops at the right wall, as shown in Fig. 10(c).

Fig. 11 is a comparison of the present investigation with that of the previous work of Umavathi and Shekar [6] by substituting $M = 0$, $Br = 0$, $\sigma = 0$, $Q = 0$, $Rd = 0$, $Sc = 0$, $Sr = 0$, and $K_1 = 0$. Furthermore, numerical values for the temperature distribution have been tabulated in Table 1. The obtained results have been compared with the analytical solution of Ref. [6], and an excellent agreement has been observed.

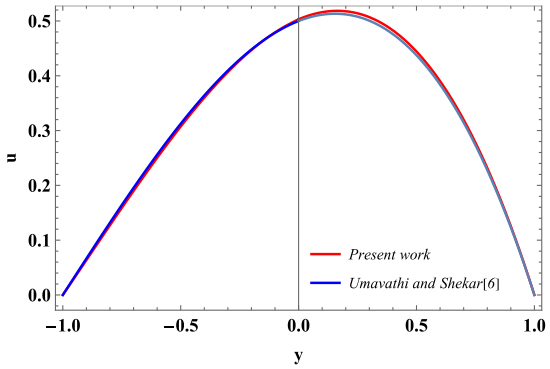

Fig. 11. Comparative study for velocity distribution of the present paper with Ref [6].

Table 1. Temperature distribution

y	Present work	Ref [6]	Error
-1	−0.312547	−0.312549	-2×10^{-6}
-0.5	0.174304	0.174311	7×10^{-6}
0	0.661156	0.661132	-2.4×10^{-5}
0.5	1.148008	1.148009	1×10^{-6}
1	1.634860	1.634830	-3×10^{-5}

5. Conclusions

This study deals with the entropy generation of two immiscible liquid flows in a vertical wavy porous space along with traveling thermal waves. couple- stress fluid and viscous liquid are occupied in Regions I and II, respectively. The results for several parameters, such as Brinkmann number, heat generation or absorption, Hartmann number, porosity parameter, Grashof number, local mass Grashof number, first-order chemical reaction parameter, Schmidt number, Soret number, and Bejan number are presented graphically and discussed. The following are the important findings:

1. The velocity distribution reduces as the wall waviness, porous parameter, and Hartmann number increase.
2. By raising the Grashof number, couple- stress fluid parameter, and heat generation(absorption) parameter, the fluid's velocity is enhanced.
3. The temperature distribution escalates as the Brinkman number and heat generation (absorption) parameter rises. Further, it falls by enhancing porous parameter and Hartmann number.
4. There is a reduction in the concentration distribution with an increase in the Schmidt number, chemical reaction parameter, and Soret number.
5. Entropy generated rises as the Brinkman number increase and it reduces as the Hartmann number, porosity parameter, and chemical reaction are increased.
6. Bejan number escalates with the rise of Hartmann number, porosity parameter, and chemical reaction and falls with the rise of Brinkman number.
7. Shear stress rises with the increase of Gr_t number whereas decreases with the Hartmann number and porous parameter at the right wall of the channel.
8. The increase in heat generation (absorption) results in an increase in the Nusselt number and In contrast, increasing the porosity parameter and Hartmann number causes a drop in the Nusselt number at the left wall of the channel.
9. Sherwood number at the right wall rises with the first order chemical reaction, Schmidt number, and Soret number.
10. The findings of the current study have been compared with that of Umavathi and Shekar [6] and an excellent agreement was found between the outcomes.

Nomenclature

p_1	Pressure of region- I $\left(N\,m^{-1}\right)$
p_2	Pressure of region -II $\left(N\,m^{-1}\right)$
$\varepsilon = \frac{a_1}{h}$	Amplitude

ρ_1	Density of region –I $\left(kg/m^3\right)$
ρ_2	Density of region –II $\left(kg/m^3\right)$
β_{t_1}	Thermal expansion of region –I $\left(K^{-1}\right)$
β_{t_2}	Thermal expansion of region –II $\left(K^{-1}\right)$
β_{c_1}	Coefficient of expansion of concentration of region –I
β_{c_2}	Coefficient of expansion of concentration of region –II
μ_1	Viscosity of region –I $\left(kg.m^{-1}.s^{-1}\right)$
μ_2	Viscosity of region –I $\left(kg.m^{-1}.s^{-1}\right)$
k_1	Thermal conductivity of region –I $\left(W/mK\right)$
k_2	Thermal conductivity of region –II $\left(W/mK\right)$
n	Ratio of density
m	Ratio of viscosity
k	Ratio of electrical conductivity
s	Ratio of thermal expansion
h	Ratio of height
D	Ratio of diffusivity
β_t	Ratio of thermal expansion
β_c	Ratio of expansion of concentration
Gr_t	Grashof number
Gr_c	Local Grashof number
M	Hartmann number
σ	Porous parameter
Br	Brinkman number
a	Couple stress fluid parameter
Pr	Prandtl number
Sc	Schmidt number
Sr	Soret number
K_1	Chemical reaction
Rd	Thermal Radiation
$L=\frac{RD\,\Delta C}{C_0}$	Diffusion parameter
R	Gas constant
D	Diffusion constant
$\delta=\frac{\Delta T}{T_0},$	Temperature difference
$\xi=\frac{\Delta C}{C_0}$	Concentration difference

Funding Statement

This research did not receive any specific grant from funding agencies in the public, commercial, or not-for-profit sectors.

Conflicts of Interest

The author declares that there is no conflict of interest regarding the publication of this article.

References

[1] Shankar, P.N. and Sinha, U.N., 1976. The Rayleigh problem for a wavy wall. *Journal of Fluid Mechanics*, *77*(2), pp.243-256.

[2] Lessen, M. and Gangwani, S.T., 1976. Effect of small amplitude wall waviness upon the stability of the laminar boundary layer. *The Physics of Fluids*, *19*(4), pp.510-513.

[3] Vajravelu, K., 1989. Combined free and forced convection in hydromagnetic flows, in vertical wavy channels, with travelling thermal waves. *International journal of engineering science*, *27*(3), pp.289-300.

[4] Vajravelu, K. and Sastri, K.S., 1980. Natural convective heat transfer in vertical wavy channels. *International Journal of Heat and Mass Transfer*, *23*(3), pp.408-411.

[5] Muthuraj, R., Srinivas, S. and Selvi, R.K., 2013. Heat and mass transfer effects on MHD flow of a couple-stress fluid in a horizontal wavy channel with viscous dissipation and porous medium. *Heat Transfer—Asian Research*, *42*(5), pp.403-421.

[6] Umavathi, J.C. and Shekar, M., 2011. Mixed convective flow of two immiscible viscous fluids in a vertical wavy channel with traveling thermal waves. *Heat Transfer—Asian Research*, *40*(8), pp.721-743.

[7] Umavathi, J.C. and Shekar, M., 2015. Unsteady mixed convective flow confined between vertical wavy wall and parallel flat wall filled with porous and fluid layer. *Heat Transfer Engineering*, *36*(1), pp.1-20.

[8] Bujurke, N.M. and Jayaraman, G., 1982. The influence of couple stresses in squeeze films. *International Journal of Mechanical Sciences*, *24*(6), pp.369-376.

[9] Rudraiah, N., Kalal, M. and Chandrashekara, G., 2011. Electrorheological Rayleigh–Taylor instability at the interface between a porous layer and thin shell with poorly conducting couple stress fluid. *International Journal of Non-Linear Mechanics*, *46*(1), pp.57-64.

[10] Shivakumara, I.S., Sureshkumar, S. and Devaraju, N., 2012. Effect of non-uniform temperature gradients on the onset of convection in a couple-stress fluid-saturated porous medium. *Journal of applied fluid mechanics*, *5*(1), pp.49-55.

[11] Rani, H.P. and Reddy, G.J., 2013. Soret and Dufour effects on transient double diffusive free convection of couple-stress fluid past a vertical cylinder. *Journal of Applied Fluid Mechanics*, *6*(4), pp.545-554.

[12] Zeeshan, A., Ali, Z., Gorji, M.R., Hussain, F. and Nadeem, S., 2020. Flow analysis of biconvective heat and mass transfer of two-dimensional couple stress fluid over a paraboloid of revolu tion. *International*

Journal of Modern Physics B, *34*(11), p.2050110.

[13] Umavathi, J.C., Kumar, J.P. and Chamkha, A.J., 2009. Convective flow of two immiscible viscous and couple stress permeable fluids through a vertical channel. *Turkish Journal of Engineering and Environmental Sciences*, *33*(4), pp.221-244.

[14] Srinivas, J. and Ramana Murthy, J.V., 2015. Flow of two immiscible couple stress fluids between two permeable beds. *Journal of Applied Fluid Mechanics*, *9*(1), pp.501-507.

[15] Abbas, Z., Hasnain, J. and Sajid, M., 2014. Hydromagnetic mixed convective two-phase flow of couple stress and viscous fluids in an inclined channel. *Zeitschrift für Naturforschung A*, *69*(10-11), pp.553-561.

[16] Lawanya, T., Vidhya, M., Govindarajan, A. and Siva, E.P., 2019, June. Effect of chemical reaction and heat source on oscillatory flow of couple stress fluid in wavy channel. In *AIP Conference Proceedings,* Vol. 2112, No. 1, AIP Publishing.

[17] Adesanya, S.O. and Makinde, O.D., 2012. Heat transfer to magnetohydrodynamic non-Newtonian couple stress pulsatile flow between two parallel porous plates. *Zeitschrift für Naturforschung A*, *67*(10-11), pp.647-656.

[18] Bashir S. and Sajid M., 2022. Flow of two immiscible uniformly rotating couple stress fluid layers. *Physics of Fluids*, *34*(6).

[19] Srinivasacharya D. and Kaladhar K., 2013. Soret and Dufour effects on free convection flow of a couple stress fluid in a vertical channel with chemical reaction. *Chemical Industry and Chemical Engineering Quarterly*, *19*(1), pp.45-55.

[20] Srinivas S. and Muthuraj R., 2011. Effects of chemical reaction and space porosity on MHD mixed convective flow in a vertical asymmetric channel with peristalsis. *Mathematical and Computer Modelling*, *54*(5-6), pp.1213-1227.

[21] Hayat T., Asghar S., Tanveer, A. and Alsaedi A., 2018. Chemical reaction in peristaltic motion of MHD couple stress fluid in channel with Soret and Dufour effects. *Results in physics*, *10*, pp.69-80.

[22] Devi, M.P. and Srinivas, S., 2023. Two layered immiscible flow of viscoelastic liquid in a vertical porous channel with Hall current, thermal radiation and chemical reaction. *International Communications in Heat and Mass Transfer*, *142*, p.106612.

[23] Goyal, K. and Srinivas, S., 2023. Entropy generation analysis for hydromagnetic two-layered pulsatile immiscible flow with Joule heating and first-order chemical reaction. *Case Studies in Thermal Engineering*, *47*, p.103046.

[24] Adesanya, S. O., Kareem, S.O., Falade, J.A. and Arekete, S.A., 2015. Entropy generation analysis for a reactive couple stress fluid flow through a channel saturated with porous material. *Energy*, *93*, pp.1239-1245.

[25] Reddy G. J., Kumar, M., Kethireddy, B. and Chamkha, A.J., 2018. Colloidal study of unsteady magnetohydrodynamic couple stress fluid flow over an isothermal vertical flat plate with entropy heat generation. *Journal of Molecular Liquids*, *252*, pp.169-179.

[26] Srinivas J., Murthy, J.R. and Sai, K. S., 2015. Entropy generation analysis of the flow of two immiscible couple stress fluids between two porous beds. *Computational Thermal Sciences: An International Journal*, *7*(2).

[27] Siva, T., Jangili, S. and Kumbhakar, B., 2023. Entropy generation on EMHD transport of couple stress fluid with slip-dependent zeta potential under electrokinetic effects. *International Journal of Thermal Sciences*, *191*, p.108339.